Electronic Supplementary Material (ESI) for Dalton Transactions.
This journal is © The Royal Society of Chemistry 2023

Supporting information: Resolving old problems with layered polytungstates related to the hexagonal tungsten bronze: phase formation, structures, crystal chemistry and some properties

Sergey F. Solodovnikov[a], Arkadiy B. Meshalkin[b], Aleksandr S. Sukhikh[a], Zoya A. Solodovnikova[a], Evgeniya S. Zolotova[a], Vasiliy N. Yudin[a1*], Yuliya M. Kadyrova[c], Elena G. Khaikina[c], Yuliya G. Mateyshina[d], Nikolai F. Uvarov[d], Aleksey M. Pugachev[e] and Evgeniy V. Kovtunets[c]

[a]*Nikolaev Institute of Inorganic Chemistry, Siberian Branch, Russian Academy of Sciences, Acad. Lavrentyev Ave. 3, Novosibirsk 630090, Russia*

[b]*Kutateladze Institute of Thermophysics, Siberian Branch, Russian Academy of Sciences, Acad. Lavrentyev Ave. 1, Novosibirsk 630090, Russia*

[c]*Baikal Institute of Nature Management, Siberian Branch, Russian Academy of Sciences, Sakh'yanova St. 6, Ulan-Ude, 670047, Buryat Republic, Russia*

[d]*Institute of Solid State Chemistry and Mechanochemistry, Siberian Branch, Russian Academy of Sciences, Kutateladze St. 18, Novosibirsk 630128, Russia*

[e]*Institute of Automation and Electrometry, Siberian Branch, Russian Academy of Sciences, Acad. Koptyug Ave. 1, Novosibirsk 630090, Russia*

E-mail: yudin@niic.nsc.ru

[*1] Corresponding author. Fax: +7(383) 3309489. Phone: +7(383) 3308465.
E-mail: yudin@niic.nsc.ru (V.N. Yudin).

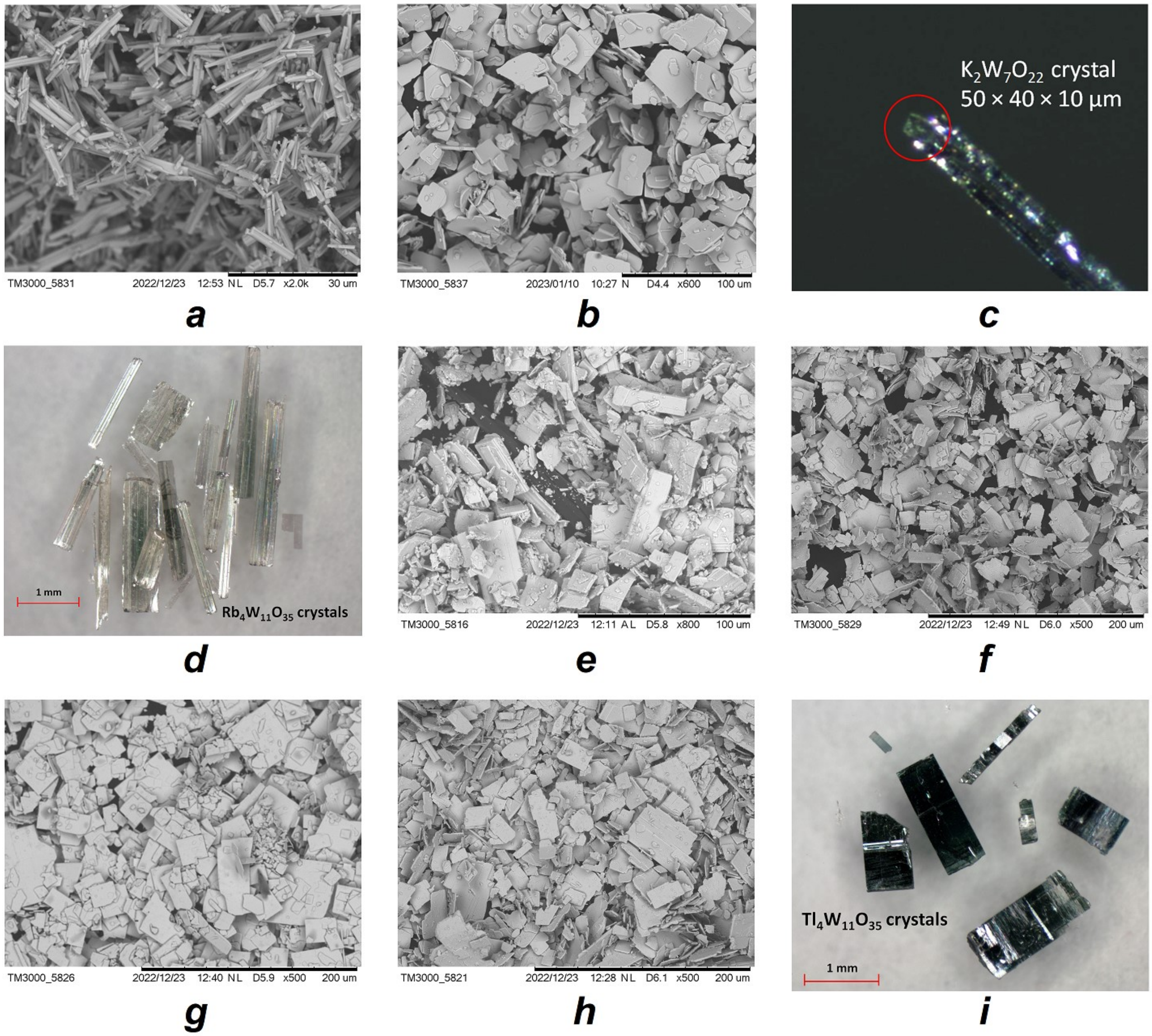

Figure S1. SEM images and photos of prepared powders and crystals of HTB-related polytungstates: (*a*) $K_4W_{11}O_{35}$ (powder); (*b*) $K_2W_7O_{22}$ (powder); (*c*) $K_2W_7O_{22}$ (crystal at a single-crystal diffractometer); (*d*) $Rb_4W_{11}O_{35}$ (crystals); (*e*) $Rb_4W_{11}O_{35}$ (powder); (*f*) $Rb_2W_7O_{22}$ (powder); (*g*) $Cs_4W_{11}O_{35}$ (powder); (*h*) $Cs_2W_7O_{22}$ (powder); (*i*) $Tl_4W_{11}O_{35}$ (crystals).

Details of the oscillation phase analysis (OPA) method

The corresponding studies were performed on an experimental setup (Fig. S2) combined the methods of OPA [1–3] and conventional thermal analysis. The method is based on that a thin platinum plate immersed in a studied liquid performs forced continuous oscillations on an elastic suspension under a harmonic force influence with a constant amplitude. When the medium state changes, the oscillation parameters of the probe plate change too. When crystals form on cooling of the sample (including crystals on the plate), the hydrodynamic resistance of the plate increases sharply, and the amplitude of the oscillations falls dramatically (Fig. S3). Thermal effects at heating can be studied using TA curves (Fig. S4). The OPA method allows one to evaluate both the melt viscosity at various temperatures and to determine the liquidus temperature along with the onset of spontaneous crystallization.

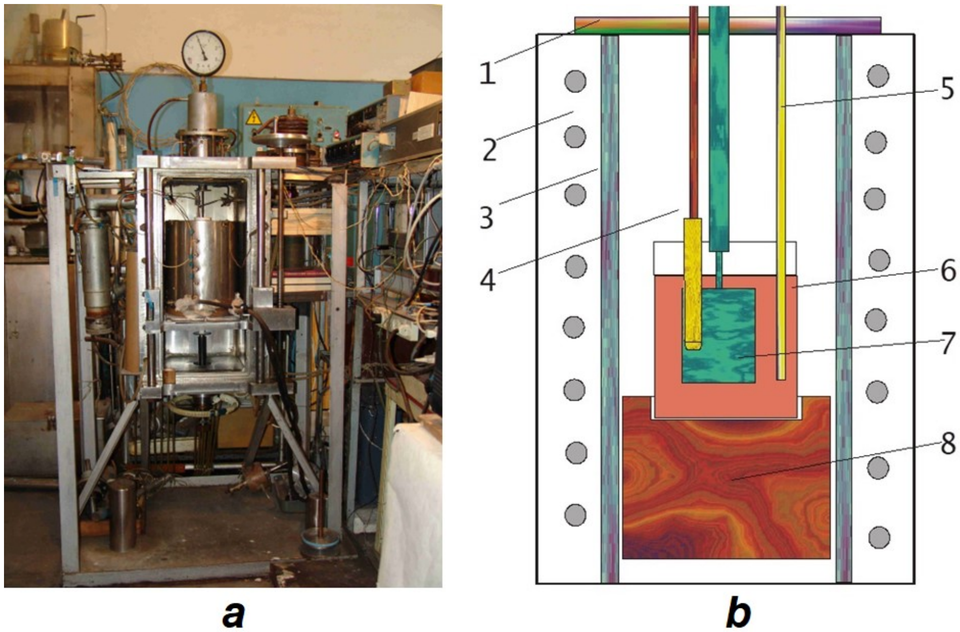

Figure S2. A general view of the OPA setup (*a*) and the scheme of the measuring cell (*b*): (1) ceramic lid; (2) high temperature resistance furnace; (3) ceramic (mullite) tube, (4) Pt-Pt/Rh thermocouple in Pt jacket; (5) Pt tube for bubbling air or other gas, (6) Pt crucible with melt; (7) viscometer probe (Pt plate); (8) ceramic support.

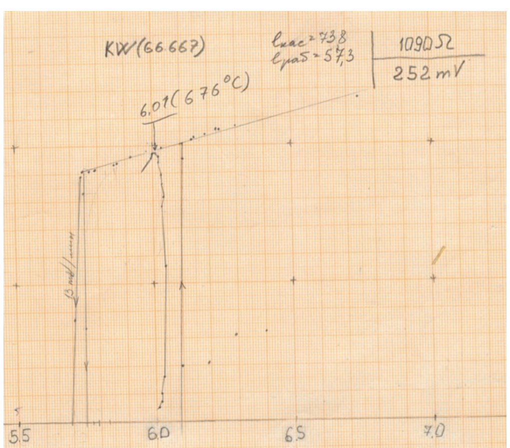

Figure S3. Oscillogram of $K_2W_2O_7$ melt at cooling and heating at 5 °C/min

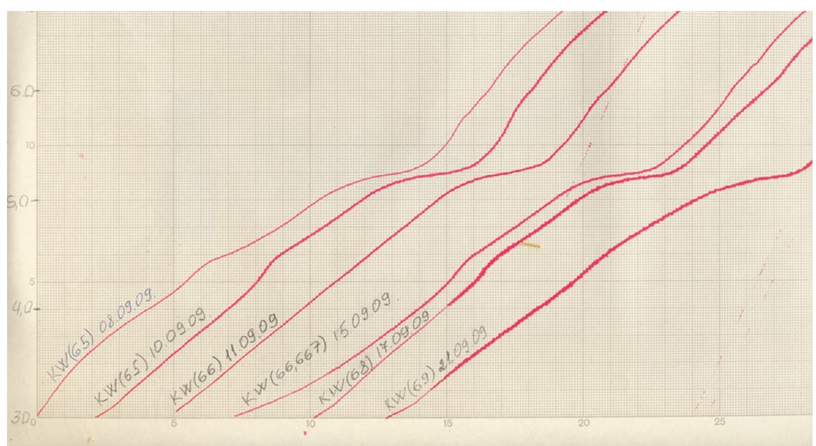

Figure S4. TA heating curves of some samples of the K_2WO_4–WO_3 system at heating rates of 5 °C/min

Phase equilibria, crystallization and melting processes in the K_2WO_4–WO_3 system were studied with the OPA method on 25 molten samples in the range of 0–72 mol% WO_3 up to 1000 °C. A platinum crucible of diameter 45 mm and height 50 mm with a pre-synthesized sample of 100-150 g mass was placed in a ceramic measuring cell heated by a furnace. The temperature of the sample was measured by a Pt-Pt/Rh thermocouple in a platinum jacket immersed in the sample melt to depth of about 20 mm. The melt height was about 30 mm. The melt homogeneity was maintained by bubbling of air through a platinum pipe. The measurement errors for the liquidus temperatures and melting points by the OPA method were no more than ± 2−3 °C [2]. To obtain additional information on phase transformations in the system, heating DTA curves were taken during the experiments at a heating rate of 5 °C/min (Fig. S4). If necessary, the probe platinum plate was removed from the melt together with crystals formed during the experiments near the liquidus temperatures for subsequent XRD identification.

References

1. A.B. Kaplun and A.B. Meshalkin, *J. Crystal Growth*, 2005, **275**, e1975–e1981.
2. A.B. Kaplun and A.B. Meshalkin, *J. Therm. Anal. Calorim*., 2008, **92**, 687–690.
3. A.B. Kaplun and A.B. Meshalkin, *High Temperature*, 2010, **48**, 527–533.

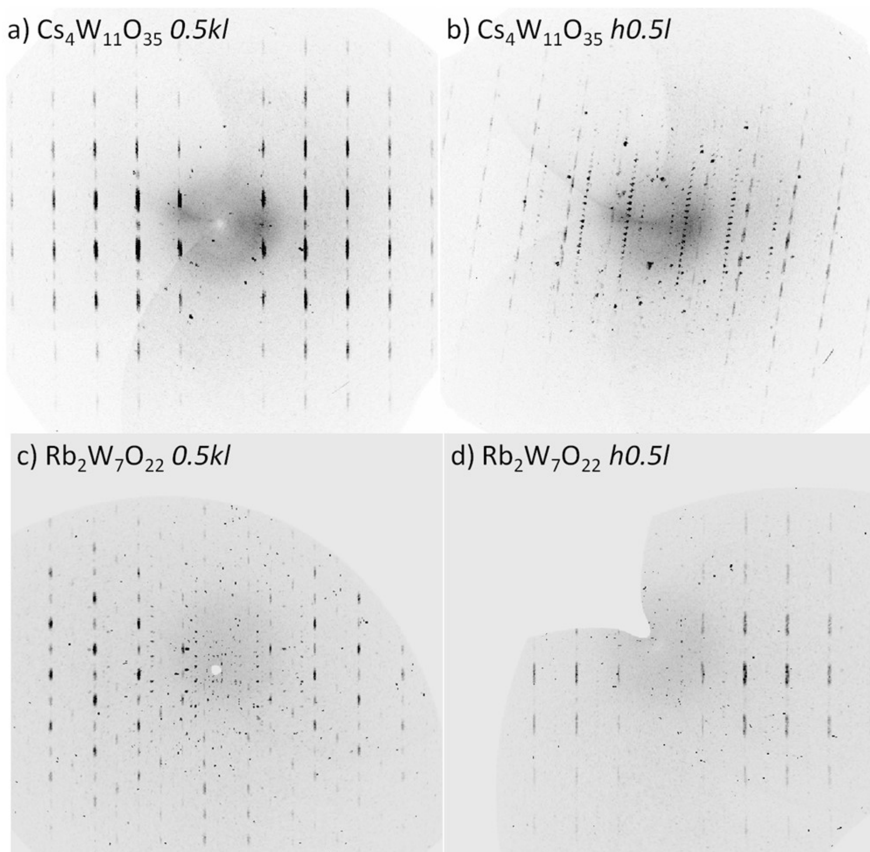

Figure S5: Precession images for *0.5kl* plane of $Cs_4W_{11}O_{35}$ (*a*), *h0.5l* plane of $Cs_4W_{11}O_{35}$ (*b*), *0.5kl* plane of $Rb_2W_7O_{22}$ (*c*) and *h0.5l* plane of $Rb_2W_7O_{22}$ (*d*).

Powder SHG Test

The SHG responses of the HTB-related polytungstates at room temperature were measured in back-scattering geometry by means of the modified Kurtz-Perry powder method. SHG signal was excited by a pulsed Nd: YAG laser (STA-01-7, Standa) with a wavelength of 1064 nm. The SHG signal at λ = 532 nm was selected by a collimator and registered by the spectrometer equipped with a CCD camera (Spec-10:256 E/LN Princeton Inst.), recorded in into a file and fit it by Lorentz contour. The integral intensity of this signal was normalized to the corresponding value of the crystalline quartz. Recording a nonlinear response with a high spectral resolution makes it possible to distinguish a narrow-band frequency SHG signal against the background of broadband noise, in particular, two-photon luminescence. This is especially relevant for recording relatively small signals.

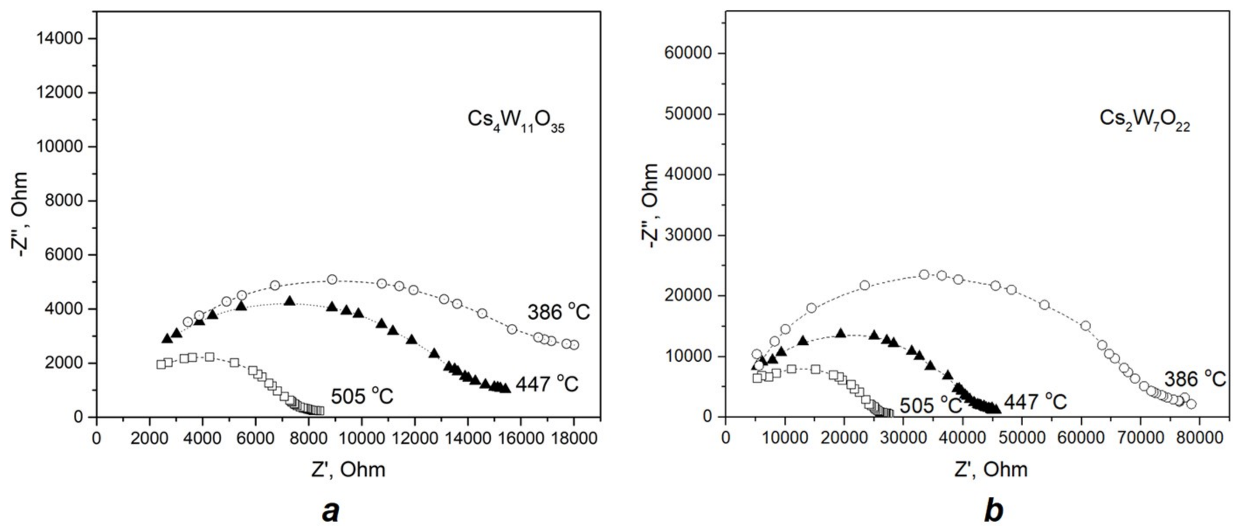

Figure S6. Nyquist plots for powder samples of $Cs_4W_{11}O_{35}$ (*a*) and $Cs_2W_7O_{22}$ (*b*) obtained at various temperatures

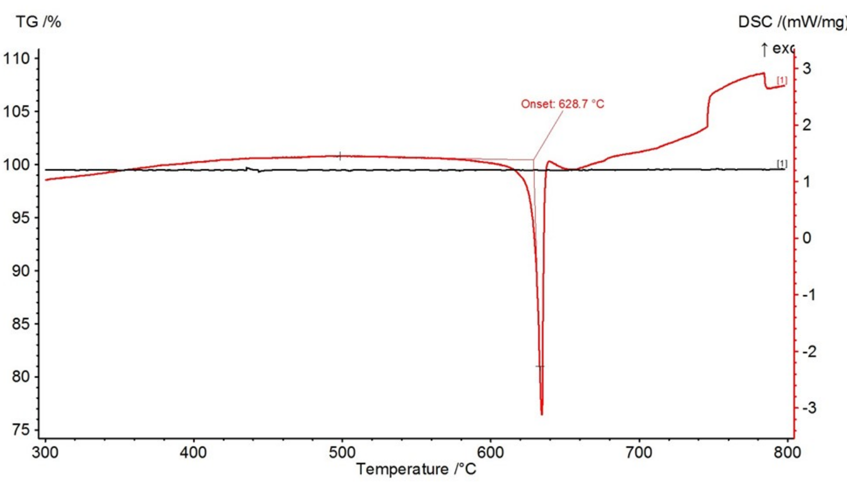

Figure S7. DSC-TG curves (STA 449 F1 Jupiter, Netzsch) of $K_2W_2O_7$

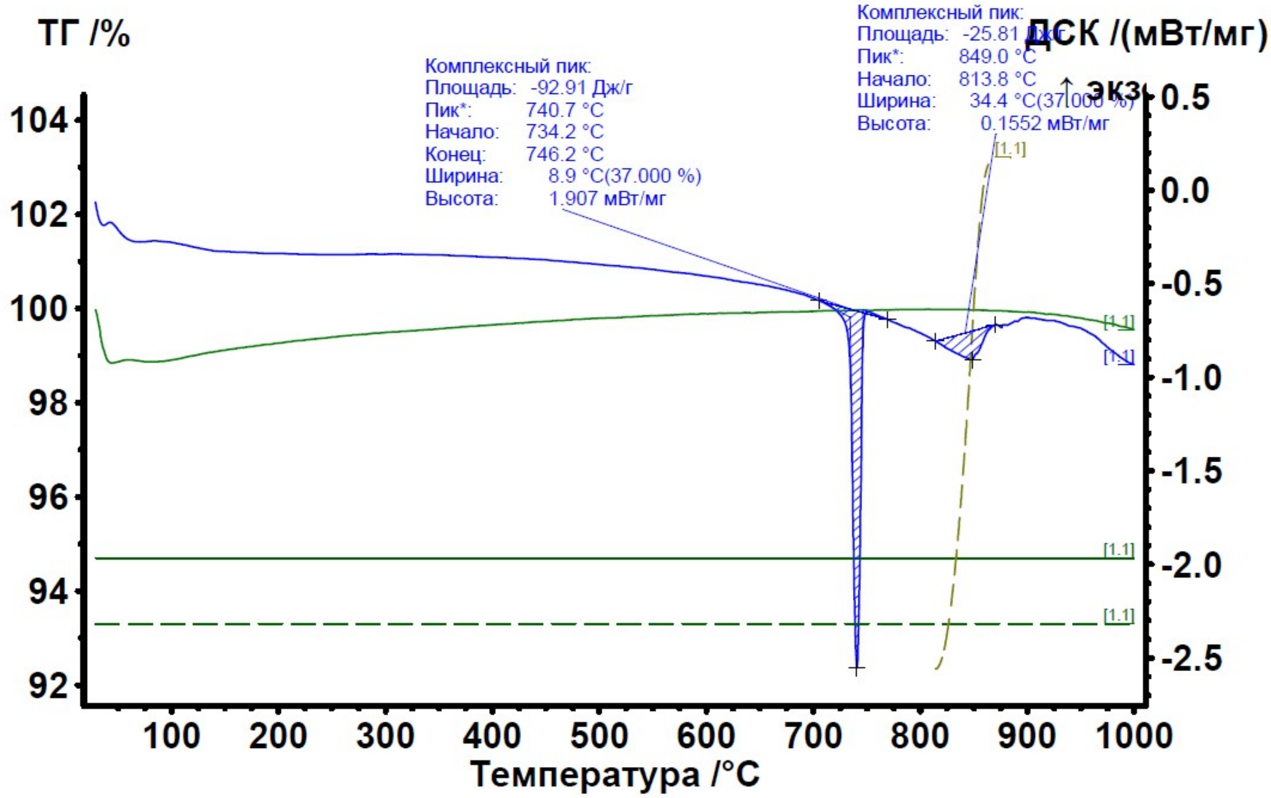

Figure S8. DSC-TG curves (STA 449 F1 Jupiter, Netzsch) of $K_2W_3O_{10}$

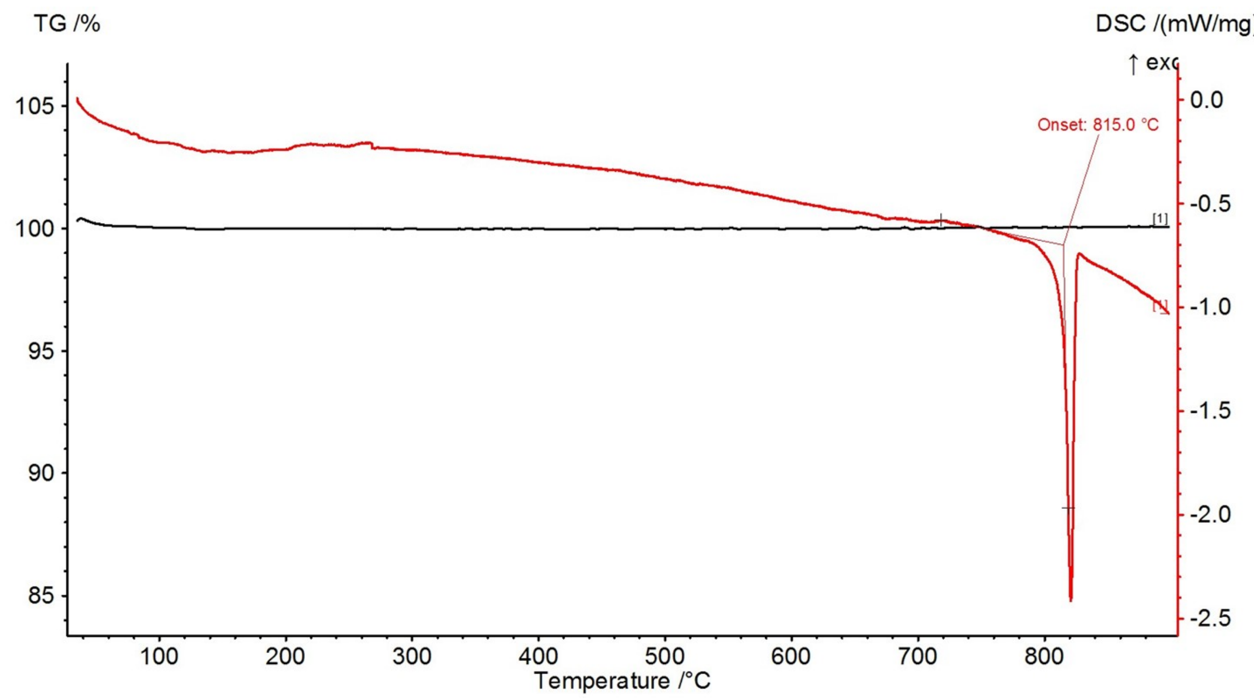

Figure S9. DSC-TG curves (STA 449 F1 Jupiter, Netzsch) of $K_2W_4O_{13}$

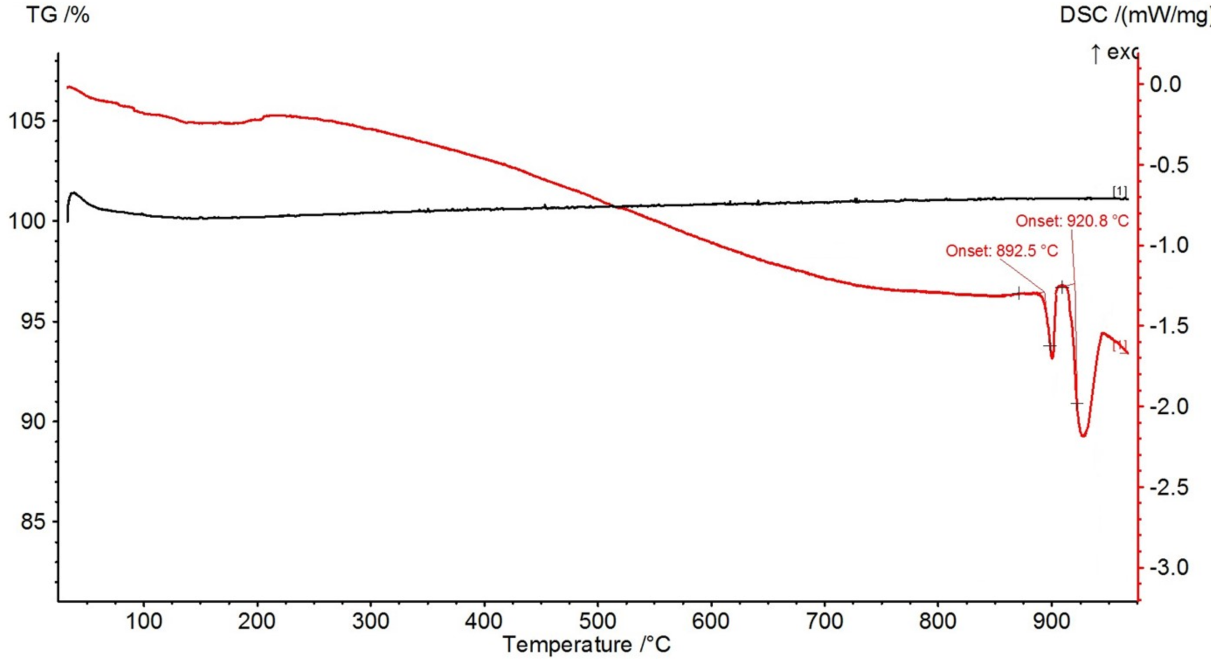

Figure S10. DSC-TG curves (STA 449 F1 Jupiter, Netzsch) of $K_4W_{11}O_{35}$

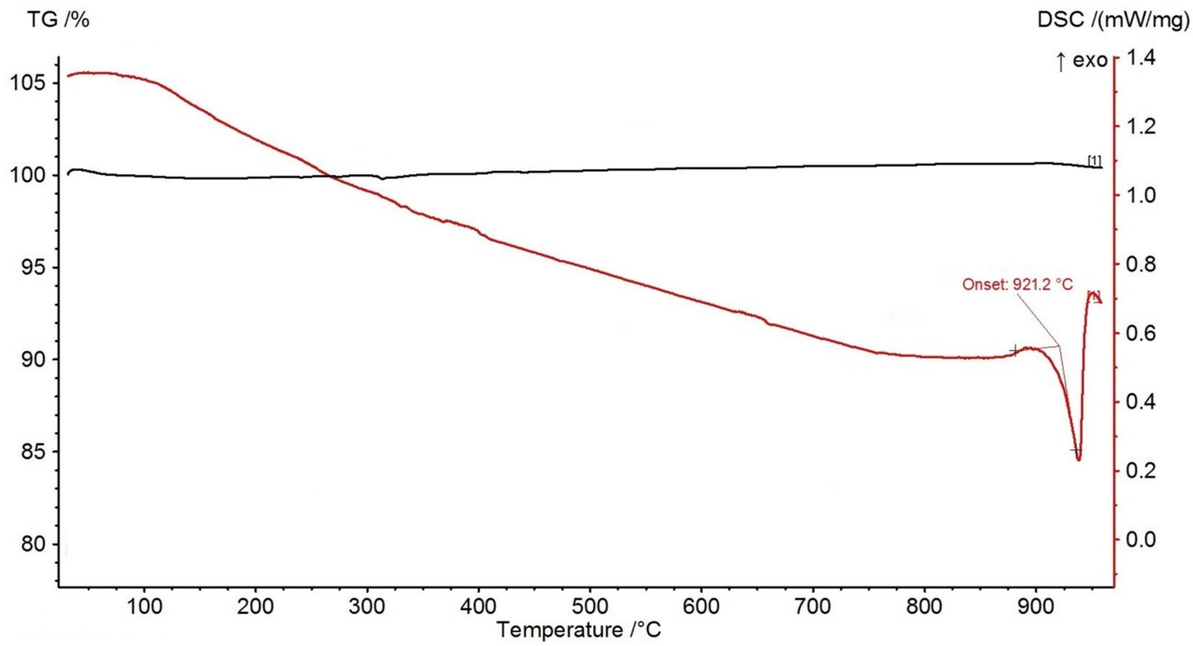

Figure S11. DSC-TG curves (STA 449 F1 Jupiter, Netzsch) of $K_2W_7O_{22}$

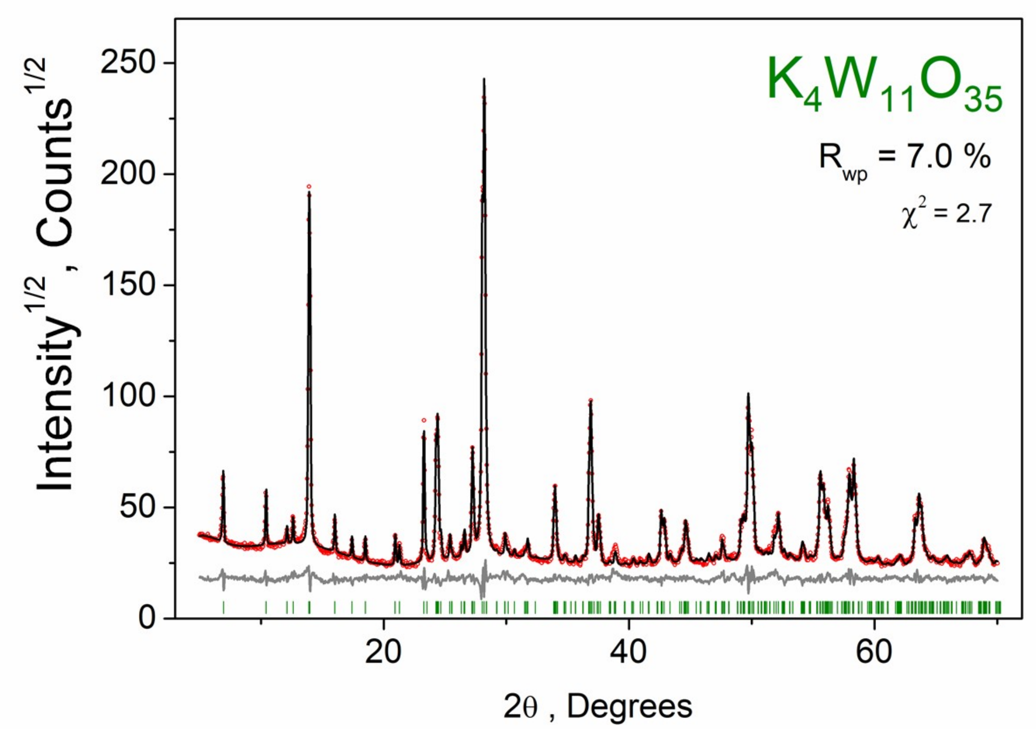

Figure S12: Observed, calculated and difference PXRD patterns of $K_4W_{11}O_{35}$

Table S1. Observed and calculated PXRD peaks for $K_4W_{11}O_{35}$

No.	2*θ* (obs.), °	*I* (obs.), %	2*θ* (calc.), °	*I* (calc.), %	*h, k, l*
1	6.928	6	6.944	5.0	0 0 2
2	10.402	4	10.424	3.1	0 0 3
3	12.109	1	12.129	0.9	0 1 0
4	12.615	2	12.619	1.4	0 1 1
5	13.938	76	13.913	41.7	0 0 4
			13.989	28.5	0 1 2
6	16.013	2	16.018	1.9	0 1 3
7	17.408	1	17.416	0.9	0 0 5
8	18.493	1	18.497	1.1	0 1 4
9	20.934	2	20.935	1.4	0 0 6
10	21.278	1	21.277	0.8	0 1 5
11	23.275	12	23.277	10.8	1 0 0
12	24.267	10	24.264	9.5	0 1 6
13	24.403	13	24.397	11.7	0 2 0
14	24.645	1	24.650	1.0	0 2 1
15	25.383	2	25.395	1.2	0 2 2
16	26.559	1	26.550	0.4	1 1 1
			26.557	0.3	–1 1 1
			26.594	0.8	0 2 3
17	27.228	10	27.196	2.9	1 0 4
			27.224	2.0	–1 0 4

			27.243	1.9	1 1 2
			27.257	2.9	–1 1 2
18	28.041	68	28.037	60.3	0 0 8
19	28.195	100	28.192	100.0	0 2 4
20	29.900	2	29.874	0.7	1 1 4
			29.899	0.6	–1 1 4
21	30.128	< 1	30.133	0.3	0 2 5
22	30.660	< 1	30.648	0.4	0 1 8
23	31.497	< 1	31.480	0.2	1 0 6
			31.516	0.1	–1 0 6
24	31.733	1	31.718	0.5	1 1 5
			31.748	0.5	–1 1 5
25	33.881	4	33.850	1.3	1 1 6
			33.883	1.3	–1 1 6
26	33.978	4	33.965	4.1	1 2 0
27	34.697	< 1	34.704	0.2	1 2 2
			34.715	0.1	–1 2 2
28	34.853	< 1	34.829	0.2	0 2 7
29	35.626	< 1	35.630	0.3	–1 2 3
30	36.753	10	36.723	3.6	1 0 8
			36.765	4.5	–1 0 8
31	36.871	16	36.855	9.1	1 2 4
			36.876	7.0	–1 2 4
32	37.151	< 1	37.131	0.6	0 3 1
33	37.440	2	37.410	1.0	0 1 10
34	37.564	2	37.500	2.9	0 2 8
35	38.843	1	38.811	0.3	1 1 8
			38.851	0.3	–1 1 8
36	38.910	1	38.911	0.3	0 0 11
37	40.332	< 1	40.343	0.3	0 2 9
38	40.898	< 1	40.905	0.2	0 1 11
39	41.591	< 1	41.577	0.3	1 1 9
			41.619	0.3	–1 1 9
40	42.604	5	42.613	4.3	0 0 12
41	42.849	3	42.855	3.0	0 3 6
42	43.338	1	43.336	0.5	0 2 10
43	44.273	1	44.278	0.3	1 3 1
			44.282	0.3	–1 3 1
44	44.503	1	44.470	0.2	0 1 12
			44.500	0.4	1 1 10
			44.544	0.3	–1 1 10
45	44.595	3	44.582	1.2	1 2 8
			44.618	1.5	–1 2 8
46	44.719	1	44.725	0.4	1 3 2
			44.734	0.3	–1 3 2
47	44.850	< 1	44.827	0.4	0 3 7

48	46.474	< 1	46.463	0.2	0 2 11
			46.485	0.2	1 3 4
			46.503	0.2	–1 3 4
49	47.081	< 1	47.070	0.2	1 2 9
50	47.577	2	47.569	1.4	2 0 0
51	49.122	3	49.084	1.7	1 0 12
			49.134	2.2	–1 0 12
52	49.321	2	49.314	1.6	1 3 6
			49.338	0.8	–1 3 6
53	49.439	1	49.413	0.3	2 1 1
			49.416	0.2	0 3 9
54	49.708	22	49.710	25.2	0 2 12
55	49.815	5	49.779	0.2	–1 2 10
			49.791	0.4	2 0 4
			49.823	0.3	2 1 2
			49.824	0.2	–2 0 4
			49.839	0.5	–2 1 2
56	50.007	13	49.997	12.4	0 4 0
57	50.144	1	50.164	0.2	0 0 14
58	51.442	< 1	51.446	0.3	2 1 4
			51.478	0.2	–2 1 4
59	51.800	2	51.810	1.9	0 1 14
60	51.993	2	51.996	1.0	0 3 10
61	52.157	4	52.157	3.9	0 4 4
62	53.120	< 1	53.085	0.2	1 3 8
			53.116	0.2	–1 3 8
63	53.323	< 1	53.345	0.2	0 4 5
64	54.067	1	54.069	0.3	1 1 13
			54.077	0.3	2 1 6
65	54.188	1	54.168	0.4	2 2 0
66	55.579	12	55.552	5.4	1 2 12
			55.598	5.7	–1 2 12
67	55.842	7	55.840	6.1	1 4 0
68	56.124	1	56.098	0.6	2 0 8
			56.158	1.0	–2 0 8
69	56.210	6	56.200	2.3	2 2 4
			56.231	1.7	–2 2 4
70	57.520	2	57.498	0.9	1 1 14
			57.550	0.6	–1 1 14
71	57.700	2	57.678	0.5	1 3 10
			57.715	0.6	–1 3 10
72	57.929	13	57.956	8.2	0 0 16
73	58.302	16	58.300	13.6	0 4 8
74	63.282	6	63.277	2.5	1 0 16
			63.333	2.3	–1 0 16
75	63.579	4	63.617	3.7	1 4 8

76	63.640	5	63.645	4.0	–1 4 8
77	63.791	2	63.815	2.2	0 2 16
78	64.226	1	64.241	0.7	0 5 2
79	64.728	1	64.700	0.2	1 1 16
			64.755	0.1	–1 1 16
80	64.806	< 1	64.823	0.2	0 5 3
81	65.779	< 1	65.796	0.2	–2 0 12
82	67.735	1	67.742	0.9	0 4 12
83	67.910	< 1	67.919	0.3	0 5 6
84	68.905	2	68.876	1.2	1 2 16
			68.930	1.2	–1 2 16

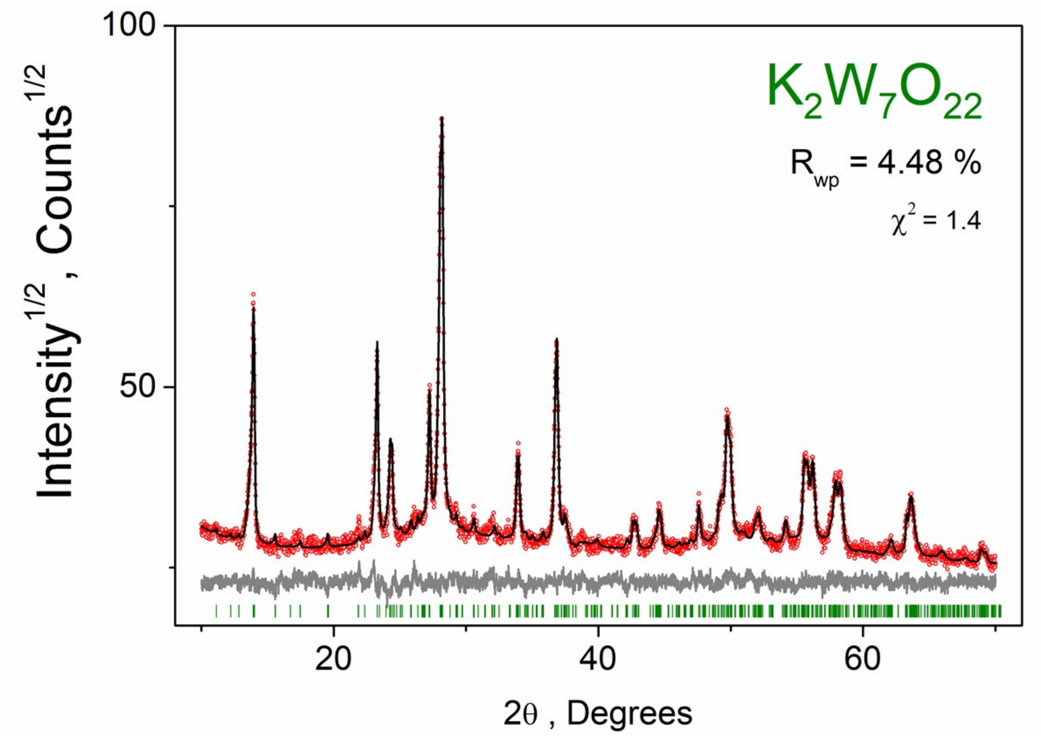

Figure S13: Observed, calculated and difference PXRD patterns of $K_2W_7O_{22}$

Table S2. Observed and calculated PXRD peaks for $K_2W_7O_{22}$

No.	**2*θ* (obs.), º**	***I* (obs.), %**	**2*θ* (calc.), º**	***I* (calc.), %**	***h, k, l***
1	11.109	1	11.120	0.7	0 0 4
2	12.179	< 1	12.202	0.4	1 0 0
			12.207	0.1	–1 0 1
3	13.951	66	13.912	26.0	0 0 5
			13.973	12.6	1 0 2
			13.996	12.6	–1 0 3
4	17.455	1	17.442	0.3	1 0 4
			17.476	0.5	–1 0 5

5	19.544	1	19.523	0.9	0 0 7
			19.557	0.6	1 0 5
6	21.829	< 1	21.837	0.3	1 0 6
7	21.918	1	21.876	0.4	–1 0 7
8	23.285	42	23.271	34.8	0 1 0
9	24.258	9	24.239	5.4	1 0 7
			24.280	5.3	–1 0 8
10	24.378	8	24.388	11.0	–2 0 1
11	27.227	23	27.213	12.7	0 1 5
			27.245	6.0	1 1 2
			27.258	5.3	–1 1 3
12	28.028	61	28.034	53.5	0 0 10
13	28.183	100	28.160	100.0	2 0 4
			28.207		–2 0 6
14	29.229	2	29.230	1.1	1 1 4
			29.251	0.6	–1 1 5
15	30.592	2	30.554	0.5	0 1 7
			30.576	0.4	1 1 5
			30.600	1.3	–1 1 6
16	32.114	1	32.125	0.6	1 1 6
			32.152	1.0	–1 1 7
17	33.868	9	33.851	3.6	1 1 7
			33.881	4.9	–1 1 8
18	33.960	13	33.961	8.6	–2 1 1
19	36.739	23	36.744	18.1	0 1 10
20	36.863	32	36.843	17.1	2 1 4
			36.880	17.4	–2 1 6
21	37.402	2	37.382	0.5	1 0 12
			37.428	0.8	–1 0 13
22	37.499	4	37.455	1.7	2 0 9
			37.529	1.6	–2 0 11
23	37.768	2	37.755	0.3	1 1 9
			37.790	0.6	–1 1 10
24	42.608	4	42.608	3.7	0 0 15
25	42.861	3	42.805	1.9	3 0 6
			42.878	2.1	–3 0 9
26	44.579	6	44.540	0.9	–1 1 13
			44.563	1.8	2 1 9
			44.627	2.0	–2 1 11
27	44.717	2	44.708	1.1	3 1 1
28	46.460	< 1	46.475	0.3	0 1 14
29	47.579	7	47.578	5.7	0 2 0
30	49.111	5	49.107	4.7	0 1 15
31	49.332	5	49.283	2.5	3 1 6
			49.308	0.9	1 2 0
			49.349	2.0	–3 1 9

32	49.693	27	49.657	12.7	2 0 14
			49.745	12.6	2 0 16
33	49.842	9	49.815	3.4	0 2 5
			49.835	1.6	1 2 2
			49.842	1.1	–1 2 3
34	49.974	14	49.978	12.7	–4 0 2
35	51.082	2	51.053	0.9	1 2 4
			51.066	0.2	–1 2 5
36	51.786	2	51.778	1.0	1 0 17
			51.828	0.8	–1 0 18
37	52.140	4	52.110	0.5	–1 1 16
			52.110	1.7	4 0 3
			52.167	1.7	–4 0 7
38	54.092	3	54.096	0.5	1 2 7
			54.117	1.7	–1 2 8
39	54.200	2	54.172	1.7	–2 2 1
40	55.560	20	55.528	9.3	2 1 14
			55.609	9.4	–2 1 16
41	55.822	12	55.824	11.4	–4 1 2
42	56.192	17	56.205	6.4	2 2 4
			56.232	6.6	–2 2 6
43	57.853	6	57.806	3.9	4 1 3
			57.859	3.4	–4 1 7
44	57.939	8	57.949	8.1	0 0 20
45	58.268	8	58.228	7.4	4 0 8
46	62.114	2	62.069	0.8	2 2 9
			62.119	1.0	–2 2 11
			62.135	0.4	4 1 7
47	63.267	7	63.300	6.4	0 1 20
48	63.534	6	63.565	6.4	4 1 8
49	63.659	7	63.665	6.3	–4 1 12
50	68.893	4	68.846	1.5	2 1 19
			68.926	0.4	3 1 16
			68.942	1.5	–2 1 21

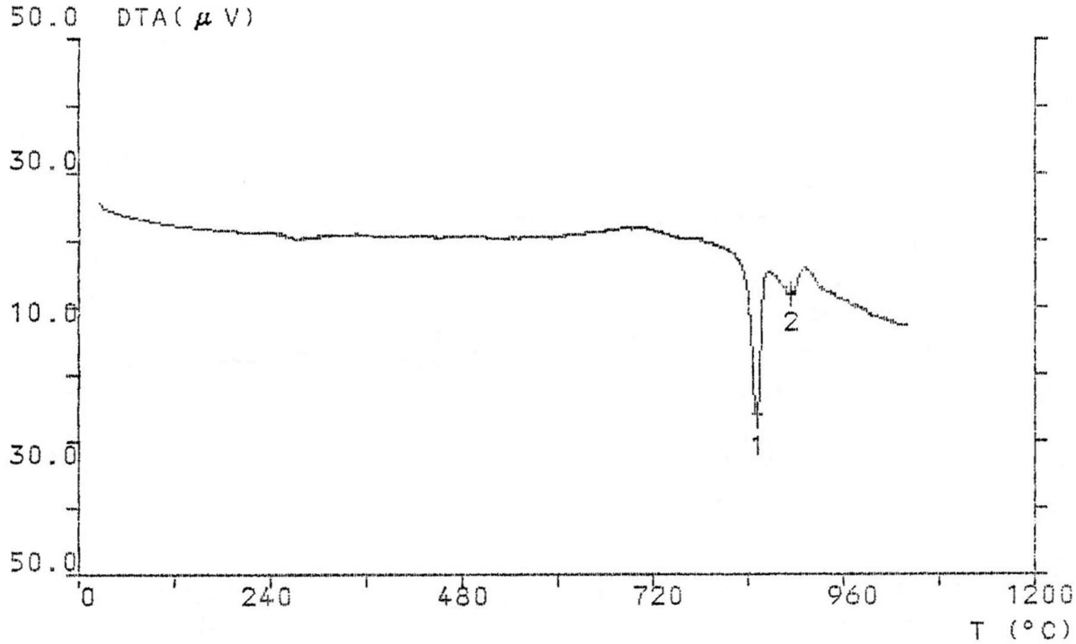

1 PEAK TEMP. [1006] [850.1 °C]
2 PEAK TEMP. [1083] [894.3 °C]

Figure S14: DTA curve (TA-7000, Hitachi) of $Rb_2W_3O_{10}$

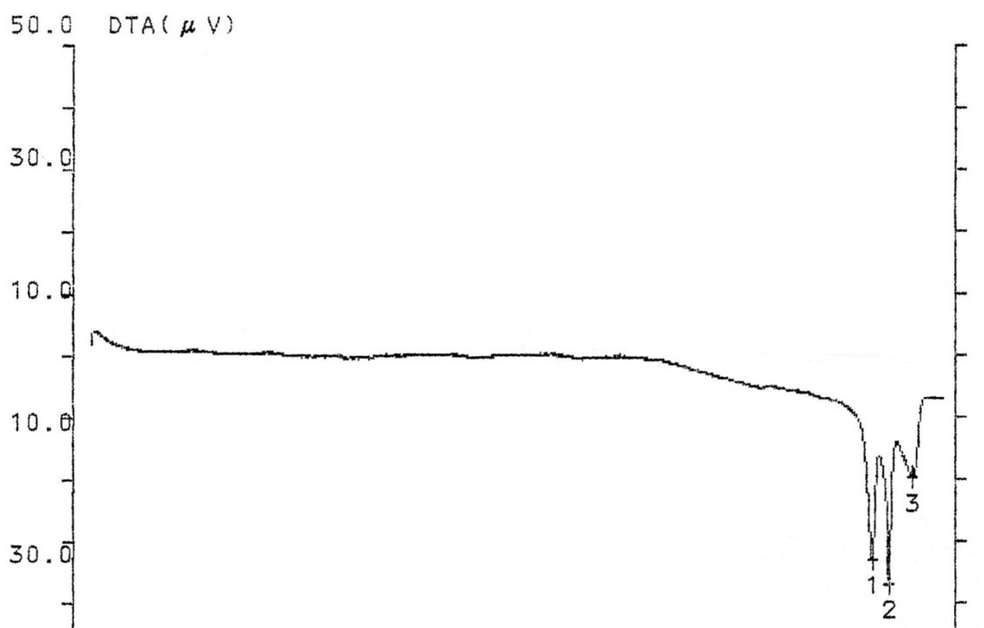

1 PEAK TEMP. [1196] [996.5 °C]
2 PEAK TEMP. [1222] [1017.2 °C]
3 PEAK TEMP. [1255] [1045.6 °C]

Figure S15: DTA curve (TA-7000, Hitachi) of $Rb_4W_{11}O_{35}$

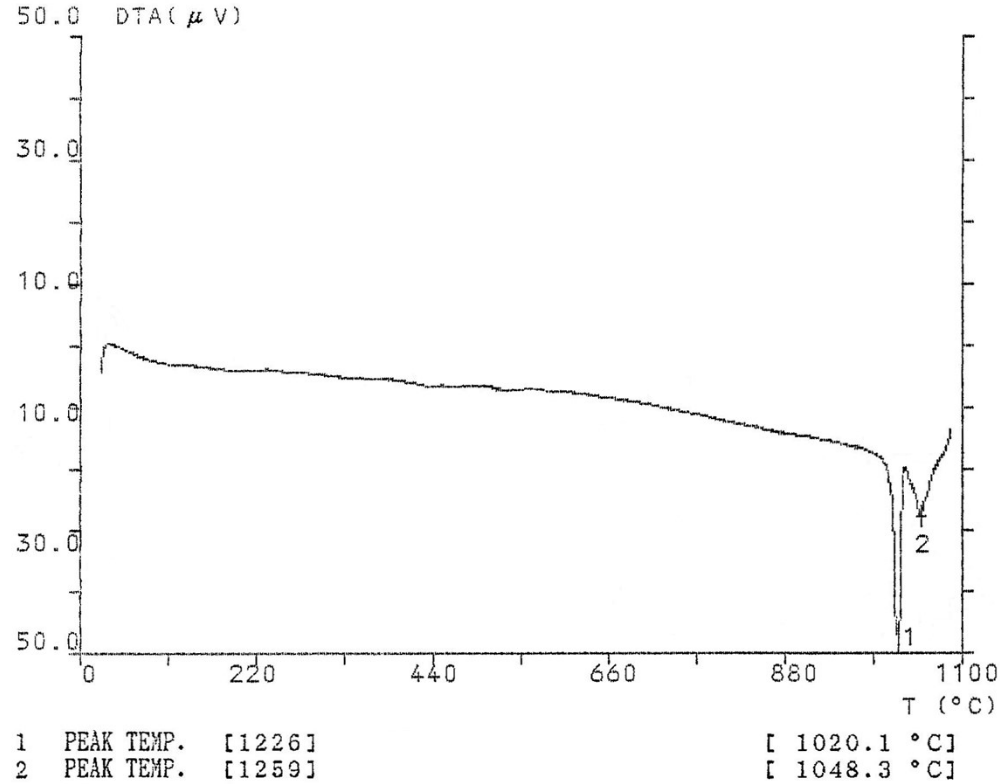

Figure S16: DTA curve (TA-7000, Hitachi) of $Rb_2W_7O_{22}$

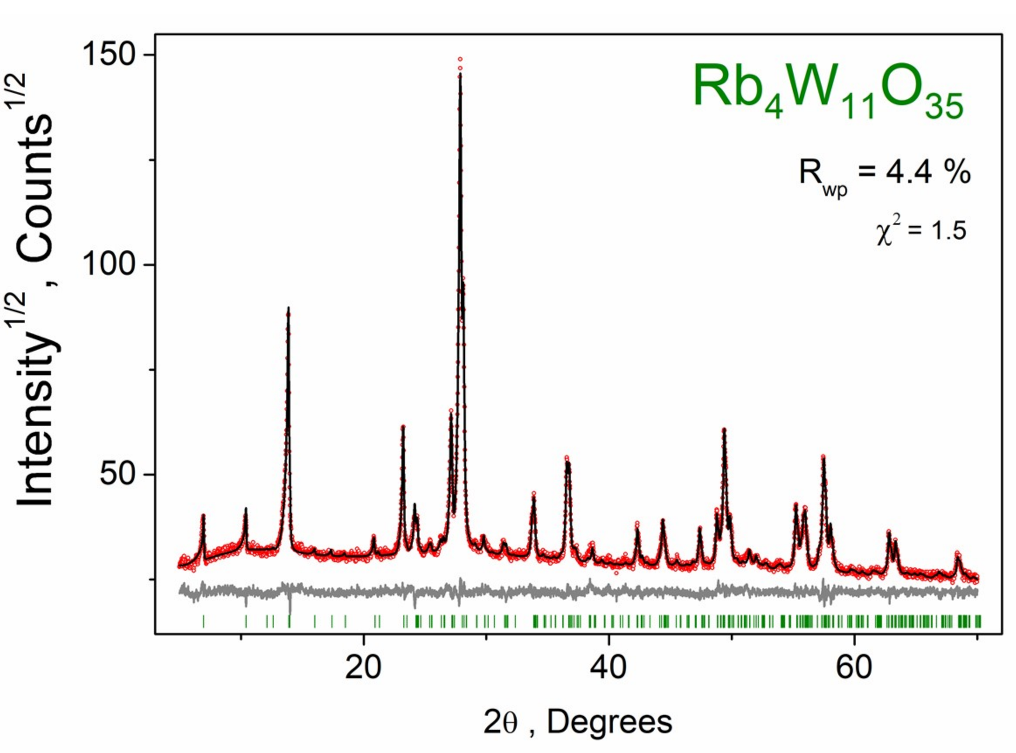

Figure S17: Observed, calculated and difference PXRD patterns of $Rb_4W_{11}O_{35}$

Table S3. Observed and calculated PXRD peaks for $Rb_4W_{11}O_{35}$

No.	2*θ* (obs.), º	*I*, %	2*θ* (calc.), º	*I*, %	*h, k, l*
1	6.881	4	6.886	3.9	0 0 2
2	10.330	4	10.337	3.7	0 0 3
3	13.824	40	13.797	32.3	0 0 4
4	15.918	1	15.924	0.5	0 1 3
5	20.762	2	20.759	1.4	0 0 6
6	23.166	13	23.163	13.1	1 0 0
7	24.081	3	24.086	3.7	0 1 6
8	24.295	3	24.297	2.6	0 2 0
9	25.289	1	25.282	0.4	0 2 2
10	25.420	1	25.412	0.5	1 0 3
11	26.211	1	26.191	0.7	1 1 0
12	26.433	2	26.424	0.5	1 1 1
13	27.067	14	27.049	5.9	1 0 4
			27.050	5.9	–1 0 4
			27.112	2.5	1 1 2
			27.113	2.2	–1 1 2
14	27.806	100	27.800	100.0	0 0 8
15	28.049	36	28.042	36.9	0 2 4
16	29.040	1	29.028	1.3	–1 0 5
17	29.716	2	29.718	0.6	1 1 4
			29.719	0.7	–1 1 4
18	29.961	1	29.958	0.2	0 2 5
19	31.320	1	31.289	0.2	1 0 6
			31.291	0.2	–1 0 6
			31.359	0.6	0 0 9
20	31.539	1	31.543	0.7	1 1 5
21	33.663	2	33.653	1.0	1 1 6
			33.654	1.3	–1 1 6
22	33.821	5	33.809	5.0	1 2 0
23	36.488	9	36.480	4.4	1 0 8
			36.482	4.8	–1 0 8
24	36.690	7	36.674	4.6	1 2 4
			36.675	4.7	–1 2 4
25	37.253	1	37.235	0.7	0 2 8
26	38.570	1	38.575	1.0	0 0 11
27	42.233	3	42.242	3.4	0 0 12
28	44.322	4	44.317	1.9	1 2 8
			44.318	2.4	–1 2 8
29	47.329	3	47.321	3.6	2 0 0
30	48.718	6	48.716	2.5	1 0 12
			48.718	2.7	–1 0 12
31	49.098	3	49.060	0.8	1 3 6
			49.061	0.7	–1 3 6

32	49.324	20	49.327	19.0	0 2 12
33	49.785	5	49.781	4.5	0 4 0
34	51.341	2	51.363	1.6	0 1 14
35	51.901	1	51.915	1.1	0 4 4
36	55.168	7	55.165	3.6	1 2 12
			55.166	3.9	–1 2 12
37	55.619	2	55.585	1.7	1 4 0
38	55.777	4	55.772	2.0	2 0 8
			55.774	2.1	–2 0 8
39	55.905	4	55.912	2.2	2 2 4
			55.913	2.2	–2 2 4
40	57.050	1	57.052	0.8	1 1 14
			57.054	0.9	–1 1 14
41	57.412	14	57.430	14.9	0 0 16
42	57.550	2	57.566	0.6	1 4 4
			57.566	0.6	–1 4 4
43	57.950	4	57.968	5.1	0 4 8
44	62.741	4	62.716	2.5	1 0 16
45	63.284	3	63.271	1.3	1 4 8
			63.272	1.1	0 2 16
			63.272	1.3	–1 4 8
46	68.318	2	68.331	1.1	1 2 16
			68.333	1.2	–1 2 16

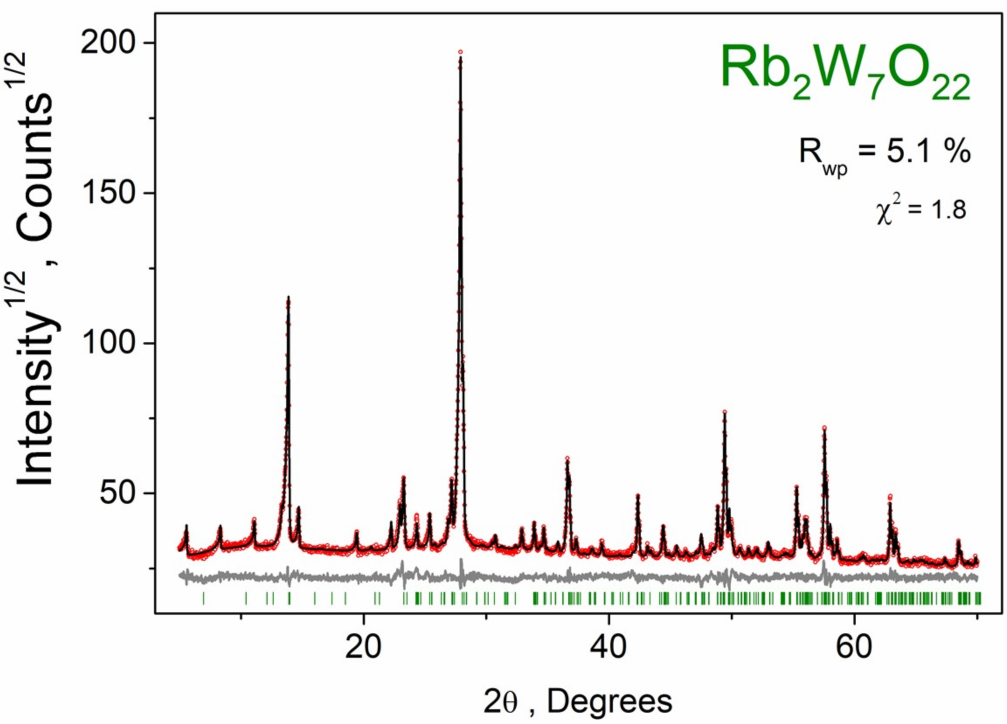

Figure S18: Observed, calculated and difference PXRD patterns of $Rb_2W_7O_{22}$

Table S4. Observed and calculated PXRD peaks for $Rb_2W_7O_{22}$

No.	2*θ* (obs.), º	*I* (obs.), %	2*θ* (calc.), º	*I* (calc.), %	*h, k, l*
1	5.530	3	5.514	2.4	0 0 2
2	8.270	2	8.276	1.9	0 0 3
3	11.042	3	11.042	2.2	0 0 4
4	13.294	2	13.280	1.2	0 1 2
5	13.820	39	13.814	40.2	0 0 5
6	14.650	3	14.654	3.0	0 1 3
7	19.394	1	19.386	1.1	0 0 7
8	22.191	1	22.188	1.8	0 0 8
9	22.900	3	22.899	2.8	0 1 7
10	23.214	7	23.214	6.6	1 0 0
11	24.279	3	24.280	1.7	0 2 0
12	25.327	2	25.333	2.4	0 1 8
13	26.816	1	26.833	0.6	1 1 2
			26.841	0.7	–1 1 2
14	27.108	4	27.103	2.8	1 0 5
			27.123	2.3	–1 0 5
15	27.842	100	27.835	100.0	0 0 10
16	28.042	18	28.040	18.1	0 2 5
17	30.431	< 1	30.407	0.2	1 0 7
18	30.674	1	30.683	0.8	0 0 11
19	32.845	2	32.824	0.6	1 1 7
			32.847	0.7	–1 1 7
20	33.852	2	33.842	1.5	1 2 0
21	34.628	2	34.614	0.7	1 1 8
			34.639	0.7	–1 1 8
22	35.755	1	35.779	0.6	0 1 12
23	36.561	7	36.535	3.1	1 0 10
			36.566	3.4	–1 0 10
24	36.722	5	36.704	2.4	1 2 5
			36.719	2.2	–1 2 5
25	37.257	1	37.265	0.8	0 2 10
26	38.499	< 1	38.524	0.3	0 1 13
27	39.359	1	39.356	0.7	0 0 14
28	42.308	4	42.297	4.5	0 0 15
29	43.387	< 1	43.371	0.4	0 3 8
30	44.368	2	44.323	0.3	1 3 2
			44.328	0.3	–1 3 2
			44.354	0.6	1 2 10
			44.380	0.8	–1 2 10
31	45.462	< 1	45.445	0.3	1 1 13
32	46.187	< 1	46.173	0.2	1 0 14
33	47.470	1	47.457	1.6	2 0 0
34	48.266	< 1	48.270	0.2	0 0 17

35	48.813	3	48.780	1.5	1 0 15
			48.817	2.0	–1 0 15
36	49.376	14	49.367	14.6	0 2 15
33	49.752	2	49.746	2.5	0 4 0
37	49.944	2	49.946	0.9	0 1 17
38	51.314	< 1	51.308	0.4	0 0 18
39	51.894	< 1	51.884	0.2	0 4 5
40	52.021	< 1	52.023	0.4	0 2 16
41	52.912	1	52.914	0.9	0 1 18
42	55.233	5	55.215	2.6	1 2 15
			55.249	2.9	–1 2 15
43	55.585	1	55.583	0.8	1 4 0
44	55.766	1	55.749	0.4	1 1 17
			55.787	0.4	–1 1 17
45	55.918	2	55.891	1.0	2 0 10
			55.936	1.0	–2 0 10
46	56.036	2	56.019	1.0	2 2 5
			56.041	0.9	–2 2 5
47	56.405	< 1	56.386	0.2	1 3 12
			56.412	0.2	–1 3 12
48	57.502	14	57.507	12.1	0 0 20
49	57.949	2	57.962	2.2	0 4 10
50	58.519	1	58.511	0.6	1 1 18
			58.549	0.5	–1 1 18
51	62.856	4	62.835	2.4	1 0 20
			62.876	2.2	–1 0 20
52	63.298	2	63.277	0.5	1 4 10
			63.298	0.5	–1 4 10
			63.337	1.0	0 2 20
53	68.420	1	68.402	0.8	1 2 20
			68.441	0.9	–1 2 20

Table S5. Atomic coordinates (×10[4]), site occupancies and equivalent isotropic displacement parameters (Å[2]×10[3]) for $K_4W_{11}O_{35}$. U_{eq} is defined as 1/3 of the trace of the orthogonalised U_{ij} tensor

Atom	Occupancy	*x/a*	*y/b*	*z/c*	U_{eq}
W(1)	0.5	5933(14)	0	-1(3)	18.6(10)
W(2)		4818(12)	7523(10)	1234.8(12)	34.1(7)
W(3)		5447(4)	2569(11)	1240.4(14)	18.7(6)
W(4)		4586(10)	5038(9)	2509.9(5)	29.2(7)
W(5)		5023(5)	2446(8)	3766.1(10)	5.4(3)
W(6A)	0.576(9)	6098(12)	7535(12)	3787.4(19)	21.1(11)
W(6B)	0.424(9)	3693(14)	7539(14)	3744(3)	21.0(15)
K(1)	0.834(4)	1040(40)	-40(50)	2539(4)	32(3)
K(2)	0.409(4)	1070(60)	4940(50)	-23(9)	18(4)
K(3)		0	70(60)	5000	56(5)
K(4)	0.258(4)	6470(80)	4950(60)	5049(15)	6(6)
O(1)	0.5	10500(300)	-630(70)	30(60)	41(19)
O(2)		5680(80)	1810(40)	510(13)	18(6)
O(3)		5750(90)	-1810(40)	511(15)	25(7)
O(4)		620(30)	7770(30)	1247(8)	-1(4)
O(5)		4310(90)	6830(40)	1930(13)	21(6)
O(6)		5580(70)	10020(50)	1420(7)	21(4)
O(7)		4730(80)	5010(50)	1006(8)	24(4)
O(8)		1140(50)	2800(30)	1214(8)	0(4)
O(9)		4400(80)	3230(40)	1924(13)	19(6)
O(10)		8800(300)	4900(300)	2370(20)	140(30)
O(11)		5500(100)	6870(50)	2948(15)	28(7)
O(12)		5720(80)	3090(40)	2968(13)	21(6)
O(13)		9500(200)	2370(90)	3630(20)	90(20)
O(14)		4270(100)	1930(50)	4422(16)	30(7)
O(15)		5460(80)	5000(50)	3855(8)	24(4)
O(16)		4570(70)	10(50)	3501(7)	17(4)
O(17)		4320(90)	8100(40)	4424(13)	19(6)
O(18A)	0.576(9)	10810(100)	7760(50)	3806(13)	-1(7)
O(18B)	0.424(9)	8810(120)	7690(80)	3670(20)	-1(9)

Table S6. Atomic coordinates (×10[4]), site occupancies and equivalent isotropic displacement parameters (Å^2×10^3) for $Rb_4W_{11}O_{35}$. U_{eq} is defined as 1/3 of the trace of the orthogonalised U_{ij} tensor

Atom	Occupancy	*x/a*	*y/b*	*z/c*	U_{eq}
W(1)	0.5	6006(8)	0	4.4(19)	6.1(4)
W(2)		4443(13)	7466(10)	1229.8(12)	28.0(7)
W(3)		5352(6)	2519(10)	1221.3(11)	17.6(8)
W(4)		5477(5)	5000(9)	2491.6(5)	14.9(4)
W(5)		5083(8)	2439(8)	3742.4(11)	7.9(3)
W(6A)	0.463(14)	5953(19)	7624(14)	3755(3)	17.6(16)
W(6B)	0.537(14)	4087(17)	7494(9)	3726.7(15)	7.7(11)
Rb(1)	0.895(5)	90(20)	72(19)	2505(2)	41.8(16)
Rb(2A)	0.629(9)	0	5182(15)	0	24(3)
Rb(2B)	0.159(9)	5000	5180(30)	0	2(6)
Rb(3)	0.871(9)	0	653(13)	5000	26.5(16)
Rb(4A)	0.443(9)	0	5210(40)	5000	39(6)
Rb(4B)	0.108(9)	5000	5230(30)	5000	90(40)
O(1)		10000	680(60)	0	26(10)
O(2)		5190(110)	-1760(50)	495(15)	23(7)
O(3)		5890(100)	1810(40)	-522(13)	16(5)
O(4)		150(60)	7820(60)	1128(18)	42(11)
O(5)		4190(90)	6800(40)	1920(13)	15(5)
O(6)		4590(80)	9960(70)	1414(9)	19(4)
O(7)		4770(90)	4990(80)	999(9)	23(5)
O(8)		9770(80)	2670(40)	1304(11)	12(5)
O(9)		5160(90)	3200(50)	1882(13)	19(6)
O(10)		9940(80)	5550(30)	2484(10)	9(4)
O(11)		5100(80)	3070(40)	2915(12)	16(5)
O(12)		5820(100)	6820(40)	2962(13)	17(6)
O(13)		5590(80)	1940(50)	4349(12)	20(6)
O(14)		5160(80)	4950(60)	3813(8)	18(4)
O(15)		270(70)	2530(50)	3626(10)	15(5)
O(16)		5360(60)	-20(50)	3481(7)	10(3)
O(17)		10070(40)	7930(30)	3778(7)	-1(3)
O(18)		4860(110)	8000(50)	4399(14)	26(8)

Table S7. Atomic coordinates (×10^4), site occupancies and equivalent isotropic displacement parameters (Å^2×10^3) for $Cs_4W_{11}O_{35}$. U_{eq} is defined as 1/3 of the trace of the orthogonalised U_{ij} tensor

Atom	Occupancy	*x/a*	*y/b*	*z/c*	U_{eq}
W(1)		0	4866(16)	0	34.8(8)
W(2)		3137(5)	4670(9)	1214.6(7)	23.1(8)
W(3A)	0.70(2)	8116(7)	4181(19)	1219.4(8)	11.2(8)
W(3B)	0.30(2)	8022(14)	5600(40)	1194.4(17)	6.5(18)
W(4A)	0.54(6)	6219(4)	4220(60)	2475.0(9)	4.1(19)
W(4B)	0.46(6)	6211(6)	5420(80)	2466.8(18)	7(2)
W(5)		9426(3)	5497(9)	3721.4(6)	6.8(3)
W(6)		4293(3)	4319(10)	3710.5(5)	9.9(3)
Cs(1)	0.816(6)	5000	0	0	10.9(7)
Cs(2)	0.943(3)	1168(6)	-242(19)	2468.5(7)	25.1(7)
Cs(3)	0.648(3)	7315(17)	58(17)	4896.3(12)	58.7(17)
O(1)		0	500(300)	0	59(10)
O(2)		1550(40)	4830(50)	-502(11)	14(5)
O(3)		2110(50)	4790(60)	513(13)	22(7)
O(4)		4110(40)	4850(50)	1875(13)	17(6)
O(5)		5450(60)	4820(60)	988(5)	16(3)
O(6)		700(70)	4730(70)	1382(5)	20(3)
O(7)		3200(40)	-300(60)	1244(7)	8(3)
O(8)		8130(40)	30(60)	1113(11)	26(6)
O(9)		7710(40)	4760(50)	1869(12)	15(6)
O(10)		5990(40)	70(90)	2394(6)	16(5)
O(11)		8290(30)	4830(40)	2899(10)	7(4)
O(12)		4550(50)	4810(60)	2897(14)	28(8)
O(13)		10210(50)	5430(90)	4343(13)	38(7)
O(14)		9370(30)	200(40)	3676(6)	3(3)
O(15)		6910(60)	4800(70)	3776(4)	14(3)
O(16)		11700(60)	4860(50)	3453(5)	13(3)
O(17)		4150(30)	4680(50)	4364(8)	9(4)
O(18)		4280(40)	-60(50)	3554(9)	24(5)

Table S8. Atomic coordinates (×10^4), site occupancies and equivalent isotropic displacement parameters (Å^2×10^3) for $Tl_4W_{11}O_{35}$. U_{eq} is defined as 1/3 of the trace of the orthogonalised U_{ij} tensor

Atom	Occupancy	*x/a*	*y/b*	*z/c*	U_{eq}
W(1A)	0.87(2)	0	5990(20)	0	-0.4(7)
W(1B)	0.13(2)	0	4460(120)	0	13(6)
W(2)		3184(3)	4755(16)	1230.1(7)	16.1(5)
W(3)		8148(3)	4536(15)	1232.6(5)	9.2(4)
W(4)		6278(3)	5709(14)	2500.6(3)	8.9(4)
W(5)		9459(2)	5792(15)	3759.0(6)	5.8(2)
W(6)		4348(3)	4716(15)	3764.0(7)	7.3(3)
Tl(1)	0.884(6)	5000	0	0	59.7(14)
Tl(2)	0.882(3)	1297(7)	387(17)	2569.8(8)	44.8(6)
Tl(3)	0.676(3)	7413(12)	232(14)	4927.2(9)	50.9(11)
O(1)	0.5	700(50)	10060(90)	-50(20)	8(9)
O(2)		1530(30)	5030(50)	-508(8)	3(3)
O(3)		2060(40)	6360(100)	540(11)	25(6)
O(4)		3430(40)	210(90)	1279(10)	15(6)
O(5)		4170(40)	6170(100)	1896(12)	22(5)
O(6)		5500(50)	5170(60)	989(7)	15(4)
O(7)		740(50)	5230(70)	1421(7)	17(4)
O(8)		8000(40)	370(50)	1074(11)	20(6)
O(9)		7750(30)	5070(60)	1912(10)	11(5)
O(10)		4630(30)	5140(50)	2932(8)	5(4)
O(11)		5530(40)	10140(100)	2408(11)	25(6)
O(12)		8330(40)	6220(100)	2980(11)	23(5)
O(13)		10280(40)	6290(100)	4398(12)	24(5)
O(14)		9740(60)	10460(140)	3827(16)	43(11)
O(15)		11710(50)	5390(60)	3481(6)	12(3)
O(16)		6900(40)	5310(60)	3843(6)	11(3)
O(17)		4140(40)	5200(70)	4423(11)	17(5)
O(18)		4190(20)	170(40)	3559(8)	2(3)

Table S9. Atomic coordinates (×10⁴), site occupancies and equivalent isotropic displacement parameters (Å²×10³) for $K_2W_7O_{22}$. U_{eq} is defined as 1/3 of the trace of the orthogonalised U_{ij} tensor

Atom	Occupancy	*x/a*	*y/b*	*z/c*	U_{eq}
W(1)		2828(3)	5560(50)	988.9(6)	18.2(5)
W(2)		7975(3)	5300(50)	977.0(6)	25.4(8)
W(3)		5985(3)	4470(50)	1990.4(4)	13.5(3)
W(4A)	0.67(3)	8882(6)	5800(50)	3014.7(10)	8.3(9)
W(4B)	0.33(3)	8941(15)	4410(80)	3036(2)	18(3)
W(5)		3960(3)	4830(50)	3013.4(7)	32.1(12)
W(6)		2046(4)	4830(50)	4002.9(4)	24.0(6)
W(7)		5000	4280(50)	5000	4.7(3)
W(8)		0	5650(50)	5000	8.2(4)
K(1)		0	0	0	68(7)
K(2)	0.437(9)	5000	-130(100)	0	12(4)
K(3A)	0.572(5)	1070(60)	130(110)	1971(7)	62(7)
K(3B)	0.191(4)	660(40)	4070(110)	1974(9)	-1(5)
K(4A)	0.350(5)	3300(40)	110(100)	5977(7)	22(5)
K(4B)	0.169(5)	2950(40)	2040(100)	5982(8)	-1(4)
O(1)		2930(20)	9920(60)	937(6)	-1(3)
O(2)		2090(40)	4560(100)	444(9)	22(5)
O(3)		550(60)	5290(90)	1193(7)	25(5)
O(4)		5420(50)	5300(90)	924(7)	25(5)
O(5)		3890(40)	4610(90)	1646(8)	21(5)
O(6)		8280(40)	5930(90)	464(9)	27(6)
O(7)		7970(30)	90(70)	1074(8)	11(5)
O(8)		7610(40)	5910(90)	1610(8)	20(5)
O(9)		5840(60)	-130(120)	2070(9)	32(8)
O(10)		8030(30)	4550(90)	2467(8)	17(5)
O(11)		4380(40)	5730(100)	2471(9)	22(5)
O(12A)	0.67(3)	8810(40)	1050(100)	3066(9)	4(5)
O(12B)	0.33(3)	9390(70)	-300(160)	2935(16)	-1(9)
O(13)		6600(60)	5290(90)	3203(7)	27(5)
O(14)		11440(60)	5170(90)	2881(7)	25(5)
O(15)		9910(30)	4520(100)	3600(8)	18(5)
O(16)		4000(70)	20(150)	3050(18)	70(20)
O(17)		3580(30)	5790(90)	3597(8)	17(4)
O(18)		4040(30)	4150(110)	4435(8)	18(4)
O(19)		2570(30)	-130(90)	4038(6)	5(4)
O(20)		390(30)	5760(90)	4435(8)	15(4)
O(21)	0.5	4960(80)	-220(130)	5146(19)	22(11)
O(22)		2570(60)	5060(90)	5163(7)	23(5)
O(23)		0	600(200)	5000	62(19)

Table S10. Atomic coordinates (×10[4]), site occupancies and equivalent isotropic displacement parameters (Å^2×10^3) for $Rb_2W_7O_{22}$. U_{eq} is defined as 1/3 of the trace of the orthogonalised U_{ij} tensor

Atom	Occupancy	*x/a*	*y/b*	*z/c*	U_{eq}
W(1)		5007(9)	2480(30)	993.5(10)	19.5(10)
W(2)		4851(15)	7610(30)	996.0(9)	43(2)
W(3)		4987(14)	5090(30)	2005.6(6)	25.1(9)
W(4)		4623(5)	2640(30)	3035.4(11)	11.6(7)
W(5)		5802(6)	7560(30)	3026.1(12)	13.4(6)
W(6)		4850(20)	70(30)	4011.0(6)	44.0(15)
W(7)		4840(13)	2590(30)	5006(2)	39.7(9)
Rb(1)	0.756(4)	-110(60)	0	1986(2)	51(4)
Rb(2)	0.574(4)	180(80)	4930(30)	4016(3)	46(5)
Rb(3)	0.670(4)	490(30)	5010(50)	64(3)	81(6)
O(1)		5470(140)	2040(80)	485(17)	31(12)
O(2)		480(110)	2430(100)	1012(15)	37(13)
O(3)		4720(150)	80(100)	1205(9)	21(7)
O(4)		5070(130)	5110(90)	938(8)	14(6)
O(5)		4650(100)	3180(60)	1659(12)	9(7)
O(6)		5270(130)	8120(70)	465(15)	22(10)
O(7)		9760(100)	7420(70)	1137(13)	19(8)
O(8)		4450(110)	6940(60)	1661(13)	15(8)
O(9)		9680(140)	4700(300)	2060(30)	150(40)
O(10)		5240(110)	3260(60)	2485(12)	9(7)
O(11)		5480(120)	6910(60)	2511(14)	14(8)
O(12)		8880(100)	2760(80)	3158(15)	33(11)
O(13)		4720(120)	5140(70)	3212(8)	12(6)
O(14)		5410(120)	90(100)	2907(10)	21(7)
O(15)		4510(130)	1890(70)	3619(16)	24(11)
O(16)		1230(80)	7780(50)	2995(9)	-1(5)
O(17)		4690(110)	8270(60)	3625(14)	16(9)
O(18)		490(180)	650(70)	4058(14)	31(13)
O(19)		5330(110)	-1720(60)	4430(13)	14(8)
O(20)		5480(140)	1830(70)	4451(17)	25(11)
O(21)		9710(130)	2760(90)	4939(17)	35(13)
O(22)		4830(170)	5100(110)	4838(10)	24(7)

Table S11. Atomic coordinates (×10[4]), site occupancies and equivalent isotropic displacement parameters ($Å^2 \times 10^3$) for $Cs_2W_7O_{22}$. U_{eq} is defined as 1/3 of the trace of the orthogonalised U_{ij} tensor

Atom	Occupancy	*x/a*	*y/b*	*z/c*	U_{eq}
W(1)		4784(10)	2450(20)	1023(2)	15.5(12)
W(2)		5030(20)	7580(20)	1036(2)	50(3)
W(3)		5040(20)	5040(20)	2039.5(10)	30.5(13)
W(4)		4624(9)	2570(30)	3055.5(18)	11.0(10)
W(5)		5783(11)	7490(30)	3049.5(19)	17.1(11)
W(6)		5010(20)	30(30)	4021.3(10)	35.7(14)
W(7)		5100(20)	2510(30)	5000(3)	38.8(15)
Cs(1)	0.808(4)	-270(30)	0	2041(2)	30(2)
Cs(2)	0.588(4)	-300(40)	5060(30)	4032(3)	23(3)
Cs(3)	0.604(4)	460(40)	4860(40)	69(4)	60(5)
O(1)		430(110)	2550(120)	1080(20)	20(16)
O(2)		5400(130)	2130(70)	517(13)	14(13)
O(3)		5060(130)	4890(100)	1003(12)	9(10)
O(4)		5030(180)	90(120)	1246(12)	12(9)
O(5)		4740(170)	3080(100)	1700(30)	40(20)
O(6)		5510(150)	8100(70)	500(18)	12(13)
O(7)		9800(140)	7610(100)	1130(20)	9(14)
O(8)		4880(120)	6880(70)	1683(19)	-1(11)
O(9)		930(100)	4630(50)	2110(14)	-1(11)
O(10)		5640(140)	6720(70)	2510(18)	4(10)
O(11)		5560(130)	3130(60)	2527(18)	3(10)
O(12)		240(150)	2460(140)	3090(20)	16(14)
O(13)		5060(180)	5010(120)	3237(12)	12(9)
O(14)		5410(170)	-20(120)	2915(14)	21(11)
O(15)		4860(140)	1830(80)	3650(20)	12(14)
O(16)		10600(160)	7460(160)	3090(30)	34(19)
O(17)		4620(150)	8210(90)	3600(20)	20(17)
O(18)		650(110)	-120(90)	4057(12)	0(12)
O(19)		5360(140)	1760(70)	4450(20)	5(11)
O(20)		5640(160)	-1800(80)	4450(20)	17(14)
O(21)		9220(90)	2270(60)	4960(17)	-1(10)
O(22)		5100(200)	5030(150)	4847(14)	24(10)

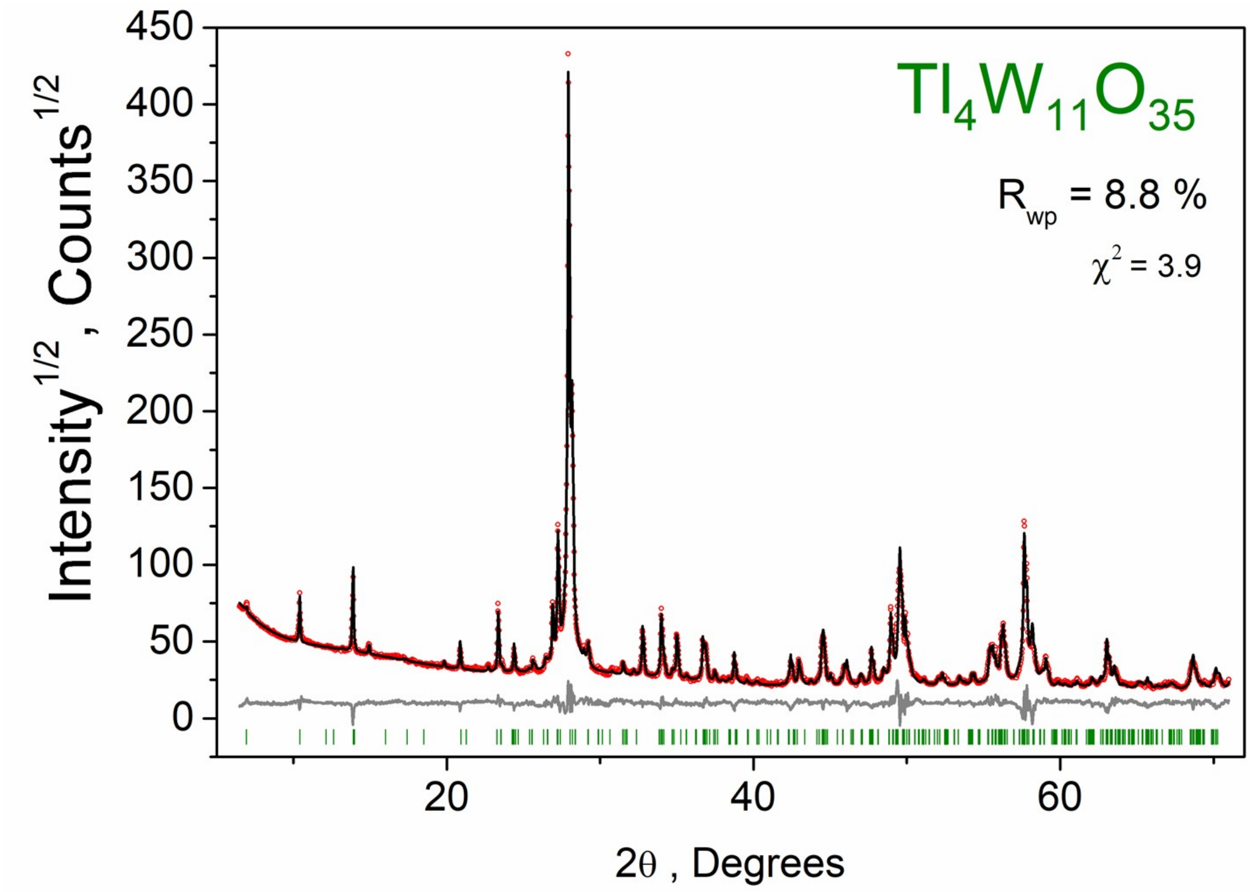

Figure S19: Observed, calculated and difference PXRD patterns of $Tl_4W_{11}O_{35}$

Table S12. Observed and calculated PXRD peaks for $Tl_4W_{11}O_{35}$

No.	2*θ* (obs.), º	*I* (obs.), %	2*θ* (calc.), º	*I* (calc.), %	*h, k, l*
1	6.909	1	6.905	0.2	2 0 0
2	10.366	2	10.369	1.6	3 0 0
3	13.837	3	13.835	3.3	4 0 0
4	14.870	< 1	14.865	0.1	2 0 1
			14.892	0.1	–3 0 1
5	19.761	< 1	19.783	0.1	–5 0 1
6	20.817	1	20.817	0.7	6 0 0
7	22.656	< 1	22.658	< 0.1	–6 0 1
8	23.299	2	23.297	2.1	0 1 0
9	23.555	< 1	23.559	0.1	1 1 0
10	24.340	< 1	24.325	0.1	–1 0 2
			24.335	0.6	7 0 0
11	25.348	< 1	25.328	< 0.1	–3 0 2
12	25.560	< 1	25.558	0.3	3 1 0
13	26.861	2	26.845	1.0	1 1 1
			26.855	1.2	–2 1 1

14	27.197	8	27.195	7.7	4 1 0
15	27.882	100	27.878	100.0	8 0 0
16	28.101	24	28.066	7.7	3 0 2
			28.113	18.2	–5 0 2
17	30.756	< 1	30.721	< 0.1	4 1 1
18	31.424	< 1	31.440	0.3	6 1 0
19	32.715	2	32.696	1.0	5 1 1
			32.724	1.0	–6 1 1
20	33.950	3	33.933	2.5	–1 1 2
21	34.137	< 1	34.114	0.2	0 1 2
			34.124	0.1	–2 1 2
22	34.681	< 1	34.643	< 0.1	6 0 2
			34.661	< 0.1	1 1 2
			34.680	< 0.1	–3 1 2
23	34.951	2	34.934	0.9	6 1 1
			34.965	0.8	–7 1 1
24	35.600	< 1	35.588	< 0.1	–4 1 2
25	36.646	1	36.639	1.4	8 1 0
26	36.789	1	36.787	0.4	3 1 2
27	36.848	1	36.824	0.7	–5 1 2
28	37.423	< 1	37.396	0.1	7 1 1
			37.430	0.2	–8 1 1
29	38.695	1	38.685	1.3	11 0 0
30	39.498	< 1	39.503	0.1	9 1 0
31	42.182	< 1	42.168	< 0.1	6 1 2
			42.226	< 0.1	–8 1 2
32	42.384	1	42.363	0.8	12 0 0
			42.415	0.1	11 0 1
33	42.871	< 1	42.874	0.3	9 1 1
34	42.917	1	42.913	0.5	–10 1 1
35	44.440	2	44.437	1.3	7 1 2
36	44.542	1	44.500	1.5	–9 1 2
37	44.991	< 1	44.962	0.2	1 1 3
38	45.866	1	45.844	0.2	10 1 1
			45.885	0.4	–11 1 1
39	46.035	< 1	46.038	0.5	–13 0 1
40	46.940	< 1	46.902	0.2	8 1 2
			46.970	0.2	–10 1 2
41	47.646	1	47.634	1.3	0 2 0
42	48.425	< 1	48.435	0.4	–7 1 3
43	48.913	3	48.902	3.1	12 1 0
44	49.409	3	49.407	3.0	11 0 2
45	49.502	7	49.494	8.0	–13 0 2
46	49.880	3	49.842	2.2	–2 0 4
			49.846	0.2	4 2 0

47	50.165	< 1	50.188	0.2	–3 2 1
48	52.277	< 1	52.264	0.3	13 1 0
49	53.379	< 1	53.401	0.1	–15 0 1
50	54.221	< 1	54.191	0.3	–1 2 2
51	55.271	< 1	55.309	0.8	11 1 2
52	55.369	1	55.389	1.0	–13 1 2
53	55.485	1	55.520	0.4	13 1 1
54	55.571	1	55.565	0.6	–14 1 1
55	55.754	1	55.711	0.3	–2 1 4
			55.732	0.2	14 1 0
56	56.123	2	56.095	1.8	8 2 0
57	56.239	2	56.202	1.0	3 2 2
			56.228	0.9	–5 2 2
			56.237	0.2	8 1 3
58	56.359	< 1	56.332	0.3	–11 1 3
59	57.631	11	57.602	13.0	16 0 0
			57.674	0.4	2 1 4
60	58.040	1	58.020	1.0	6 0 4
61	58.149	1	58.124	2.4	–10 0 4
62	58.783	< 1	58.799	0.2	–12 1 3
63	59.021	1	58.977	0.3	14 1 1
			59.024	0.7	–15 1 1
64	61.061	< 1	61.018	0.1	16 0 1
			61.070	0.1	–17 0 1
65	62.018	< 1	62.003	0.1	7 2 2
			62.053	0.2	–9 2 2
66	62.596	< 1	62.597	0.2	–16 1 1
67	63.012	2	62.983	2.2	16 1 0
68	63.483	1	63.478	0.5	–10 1 4
			63.497	0.2	–17 0 2
69	65.647	< 1	65.622	0.3	12 2 0
70	67.250	< 1	67.215	0.1	–15 1 3
71	68.499	1	68.515	0.5	15 1 2
72	68.607	1	68.610	1.2	–17 1 2

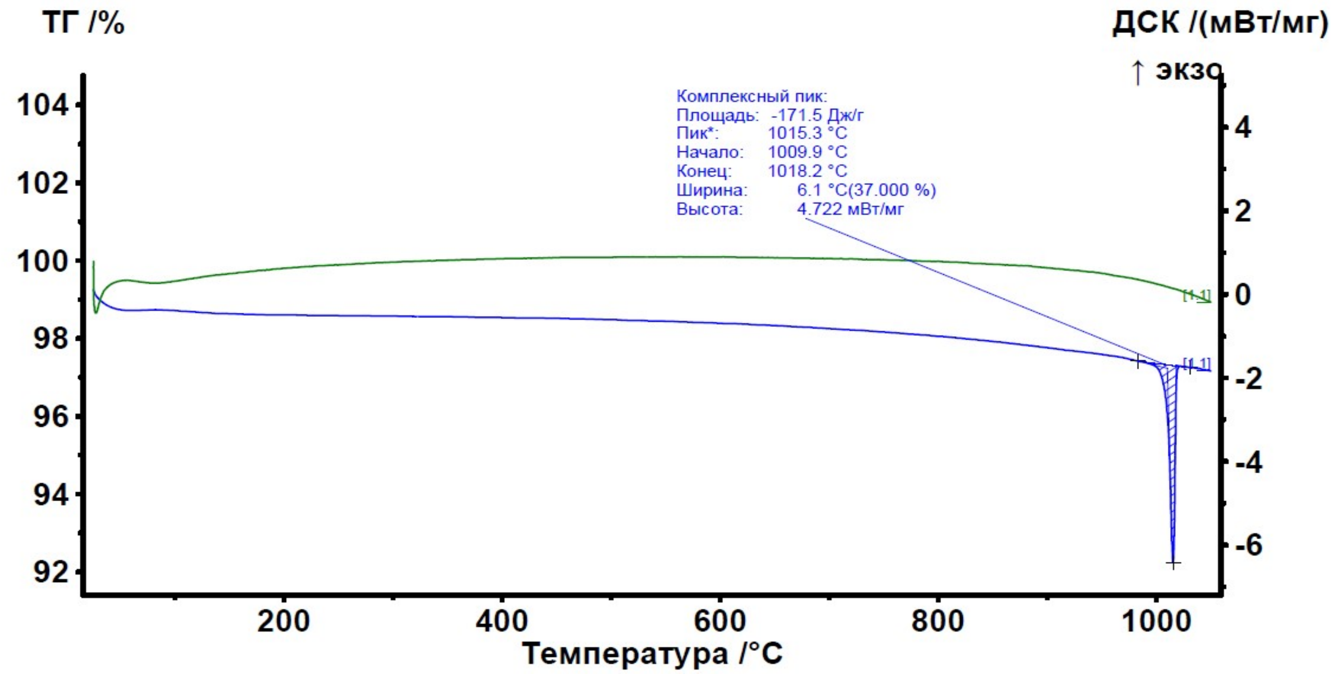

Figure S20. DSC-TG curves (STA 449 F1 Jupiter, Netzsch) of $Tl_4W_{11}O_{35}$